

FDSOI MOSFET Subthreshold Slope Model Accuracy Improvement Introducing Low-Field Quantum Mechanical Correction

Thomas Bédécarrats
Univ. Grenoble Alpes
CEA-LETI
Grenoble, France
thomas.bedecarrats@cea.fr

François Triozon
Univ. Grenoble Alpes
CEA-LETI
Grenoble, France
francois.triozon@cea.fr

Sébastien Martinie
Univ. Grenoble Alpes
CEA-LETI
Grenoble, France
sebastien.martinie@cea.fr

Mikaël Cassé
Univ. Grenoble Alpes
CEA-LETI
Grenoble, France
mikael.casse@cea.fr

Olivier Rozeau
Univ. Grenoble Alpes
CEA-LETI
Grenoble, France
olivier.rozeau@cea.fr

Abstract— This paper presents an analytical expression for the FDSOI MOSFETs subthreshold slope model accounting for low electric field quantum mechanical effect. The expression is derived from the perturbation theory applied to the system Hamiltonian considering the inversion layer carriers as particles in a one-dimensional box with an applied electric field the Hamiltonian. The effect is implemented by the introduction of a correction factor Γ_0 into the classical subthreshold slope analytical expression. Γ_0 is a function of the silicon film thickness square times temperature product and depends on the effective masses. The model is validated by its comparison with self-consistent one-dimensional Poisson-Schrödinger simulations and demonstrates unprecedented accuracy, in all studied temperature and bias range. Implemented into the inversion charge model, the correction describes better the back biasing dependence of the FDSOI MOSFET experimental subthreshold drain current.

Keywords— Semiconductor device modeling, FDSOI MOSFET, Subthreshold currents, quantum confinement

I. INTRODUCTION

Quantum Mechanical (QM) corrections must be introduced into compact models to describe properly advanced CMOS device electrical behavior, in terms of threshold voltage, gate capacitance or subthreshold slope (SS). While QM effects on symmetrical double-gate (SDG) MOSFETs have been widely studied [1]–[5], fewer works cover the asymmetrical (ADG) – and more general – device, like FDSOI MOSFETs [6]–[8]. QM correction are related to mobile carrier energy quantization and density redistribution due to either Structural or field-induced Electrical Confinements (SC and EC). These confinements are responsible for a threshold voltage shift and a gate capacitance degradation, respectively. They are generally implemented by a gates work-function shift [4]–[8] (or a bandgap broadening [2]) for the SC and an oxide thickness expanding [2], [5], [8] for the EC. EC QM corrections systematically derives from the triangular potential well approximation [9], which holds only under high electric field condition, like in strong inversion operation mode (whatever the device) or in weak inversion operation mode for highly back biased ADG MOSFETs with thin buried oxide (BOX). Concerning the SS, carrier quantization has no impact on it for SDG [1], [4] and a negligible one for thick BOX ADG MOSFETs [6]. However, as the BOX thickness decreases, QM effect on SS becomes perceptible, even at low electric field (LEF), and it has not been investigated yet. In this context, we present a proper LEF QM correction on FDSOI (i.e. arbitrary ADG) MOSFET SS classical model [10], [11], to improve prediction when compared with self-consistent one-dimensional Poisson-Schrödinger (1DPS) numerical simulation results. For the sake of clarity, we systematically consider null flat

band voltages, and the absence of interface traps and oxide charges. We study long and large device to get ride from short channel effects, and n-type carriers without loss of generality.

II. QM SS MODEL

In MOSFETs in subthreshold regime, the diffusion currents dominates. Thus, the SS can be expressed from the inversion charge at the source side Q_i and the front gate voltage V_{gf} as:

$$SS = [d \log Q_i / dV_{gf}]^{-1} \quad (1)$$

In FD-SOI device (Fig. 1) and under classical assumptions, one expresses Q_i as [12]:

$$Q_i^{CL} = q_e n_i t_{si} \exp\left(\frac{\phi_+}{\phi_T}\right) \sinh\left(\frac{\phi_-}{\phi_T}\right) \frac{\phi_T}{\phi_-} \quad (2)$$

with q_e the elementary charge, n_i the intrinsic carrier density, t_{si} the silicon film thickness, ϕ_T the thermal voltage, $\phi_+ = (\phi_{sf} + \phi_{sb})/2$ and $\phi_- = (\phi_{sf} - \phi_{sb})/2$, where ϕ_{sf} and ϕ_{sb} are the front and back surface potentials respectively. These surface potentials are related to front and back gate voltages V_{gf} and V_{gb} through capacitive couplings:

$$\begin{cases} \phi_+ &= V_{g\Sigma}/2 + (k_{eq}/k_b - k_{eq}/k_f) V_{g\Delta}/2 \\ \phi_- &= k_{eq} V_{g\Delta}/2 \end{cases} \quad (3)$$

where $V_{g\Sigma} = V_{gf} + V_{gb}$ and $V_{g\Delta} = V_{gf} - V_{gb}$ are the sum and the difference of the front and back gate voltages, and $k_f = C_{fox}/C_{si}$, $k_b = C_{box}/C_{si}$ and $k_{eq}^{-1} = 1 + k_f^{-1} + k_b^{-1}$ are capacitive factors [13]. Combining (1)-(4), one can derive the “classical” SS expression:

$$SS_{CL} = 2\phi_T \ln(10) \left[1 - \frac{k_{eq}}{k_f} + \frac{k_{eq}}{k_b} + k_{eq} \left(\coth\left(\frac{k_{eq} V_{g\Delta}}{2\phi_T}\right) - \frac{2\phi_T}{k_{eq} V_{g\Delta}} \right) \right]^{-1} \quad (5)$$

In the low electric field limit ($V_{g\Delta} \rightarrow 0$), a 1st-order Taylor series expansion allows writing:

$$SS_{OCL} = 2\phi_T \ln(10) \left(1 - \frac{k_{eq}}{k_f} + \frac{k_{eq}}{k_b} + \frac{k_{eq}^2}{6\phi_T} V_{g\Delta} \right)^{-1} \quad (6)$$

Taking now a QM description of the inversion charge layer, the Q_i expression becomes [6]:

$$Q_i^{QM} = -\frac{q_e^2 n_i}{N_C \pi \hbar^2} \exp\left(\frac{\phi_+}{\phi_T}\right) \sum_{v,n} g_v m_{d,v} \exp\left(-\frac{E_{n,v}}{\phi_T}\right) \quad (7)$$

where N_C is the conduction-band density of state, \hbar the reduced Planck constant, v , g_v , $m_{d,v}$ and $E_{n,v}$ the considered valley, its degeneracy, its effective longitudinal electron masses and its n^{th} subband energy level referred to the conduction-band in the middle of the film (the sum on n goes from one to infinity). Now, from (1), (3) and (7), we can express the QM version of SS:

$$SS_{QM} = 2\phi_T \ln(10) \left(1 - \frac{k_{eq}}{k_f} + \frac{k_{eq}}{k_b}\right) + 2 \frac{\sum_{v,n} g_v m_{d,v} \exp\left(-\frac{E_{n,v}}{\phi_T}\right) \frac{dE_{n,v}}{dV_{gf}}}{\sum_{v,n} g_v m_{d,v} \exp\left(-\frac{E_{n,v}}{\phi_T}\right)} \quad (8)$$

To derive SS_{QM} in the low electric field limit, we first follow [14] to express $E_{n,v}$ applying the 2nd-order perturbation theory to the system Hamiltonian, considering the inversion layer electrons as particles in a one-dimensional box with an applied electric field F (noticing that, in subthreshold regime, $F = k_{eq} V_{g\Delta} / t_{si}$):

$$E_{n,v} = E_{n,v}^{(0)} - \Gamma_{n,v} k_{eq}^2 V_{g\Delta}^2 \quad (9)$$

$$E_{n,v}^{(0)} = \frac{\pi^2 \hbar^2 n^2}{2q_e m_{z,v} t_{si}^2} \quad (10)$$

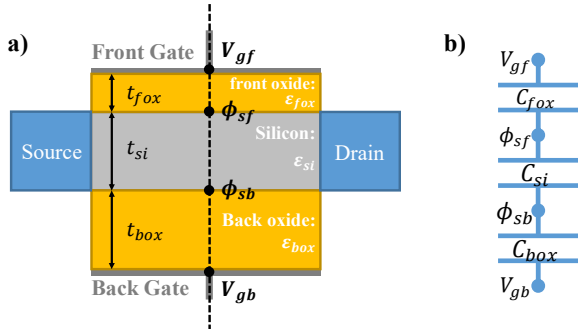


Fig. 1 a) Schematic of a FDSOI MOSFET and b) equivalent capacitive network coupling front and back gate voltages V_{gf} and V_{gb} with front and back surface potentials ϕ_{sf} and ϕ_{sb} .

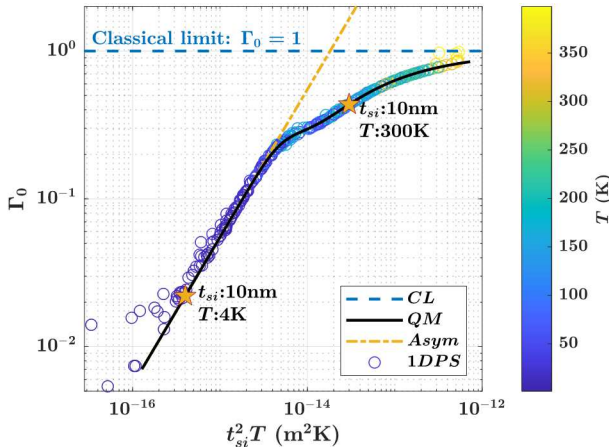


Fig. 2 Γ_0 versus $t_{si}^2 T$ extracted from 1DPS simulations, predicted by QM and CL models and the 1st subband filled only asymptote (Asym).

$$\Gamma_{n,v} = \left(\frac{15 - n^2 \pi^2}{48 n^2 \pi^2}\right) E_{n,v}^{(0)-1} \quad (11)$$

Then, from (7)-(11), after a 1st-order Taylor series expansion around $V_{g\Delta} = 0$ and a relevant rearrangement to have an expression close to (6), we get:

$$SS_{0QM} = 2\phi_T \ln(10) \left(1 - \frac{k_{eq}}{k_f} + \frac{k_{eq}}{k_b} + \frac{k_{eq}^2}{6\phi_T} V_{g\Delta} \Gamma_0\right)^{-1} \quad (12)$$

with:

$$\Gamma_0 = 24\phi_T \frac{\sum_{v,n} g_v m_{d,v} \exp(-E_{n,v}^{(0)}/\phi_T) \Gamma_{n,v}}{\sum_{v,n} g_v m_{d,v} \exp(-E_{n,v}^{(0)}/\phi_T)} \quad (13)$$

We notice that Γ_0 is a function of the $t_{si}^2 T$ product, which is consistent with the quantum level filling dependence on t_{si}^2 and T : given T , a wider t_{si}^2 brings energy levels closer (see (10)) and, given t_{si}^2 , a higher T increases the probability for electrons to reach high energies, both mechanisms filling the higher energy levels up

Comparing (6) and (12), the QM effect inclusion in the low electric field limit simply rely on a $V_{g\Delta}$ scaling by Γ_0 in the SS_0 expression (noticing that Γ_0 should tend to 1 in the classical limit):

$$SS_{0QM}(V_{g\Delta}) = SS_{0CL}(\Gamma_0 V_{g\Delta}) \quad (14)$$

We finally define the QM SS model introducing the $V_{g\Delta}$ scaling into the general SS classical formulation (5):

$$SS_{QM}(V_{g\Delta}) \equiv SS_{CL}(\Gamma_0 V_{g\Delta}) \quad (15)$$

III. MODEL VALIDATION AND DISCUSSION

To validate the model, we first compute $Q_i(V_{g\Delta})$ around $Q_i(0) = 0.1$ pC/m² with a self-consistent 1DPS solver

TABLE I
VALLEYS, DEGENERACY (g_v) AND EFFECTIVE MASSES (m_z, m_d) PER VALLEY FOR ELECTRONS FOR {100} SILICON CRYSTAL ORIENTATION

Valley	g_v	m_z/m_0	m_d/m_0
Unprimed (up)	2	0.918	0.192
Primed (p)	4	0.192	0.420

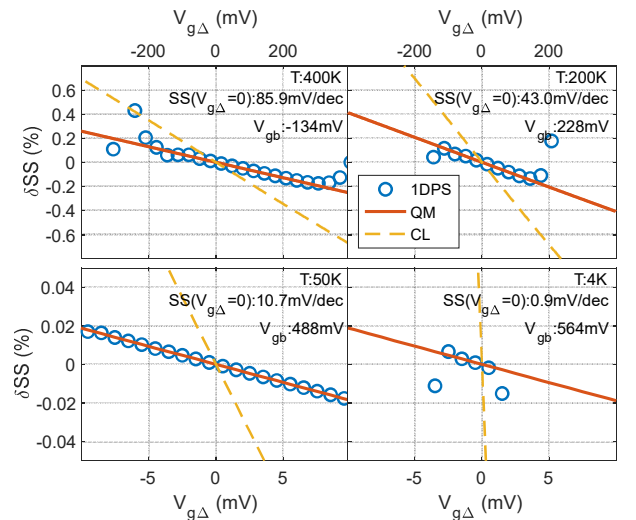


Fig. 3 δSS versus $V_{g\Delta}$ at different temperatures extracted from 1DPS and predicted by QM and CL models ($t_{fox} = 1$ nm, $t_{si} = 7$ nm and $t_{box} = 25$ nm).

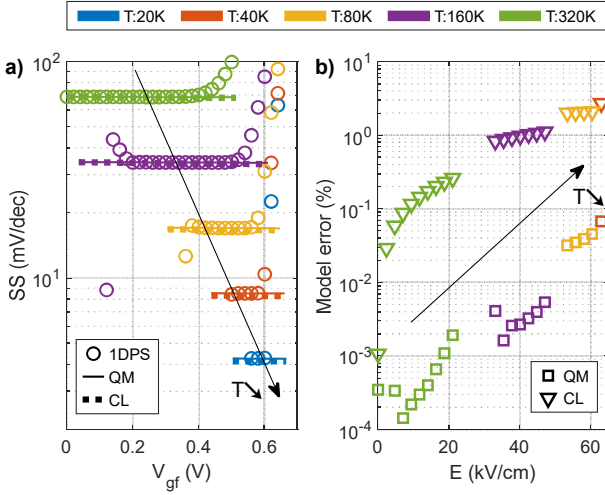


Fig. 4 (a) SS versus V_{gf} extracted from 1DPS and predicted by QM and CL models and (b) Model errors versus electrical field E , at different temperatures T at $V_{gb} = 0$ V for a typical FDSOI stack ($t_{fox} = 1$ nm, $t_{si} = 7$ nm and $t_{box} = 25$ nm).

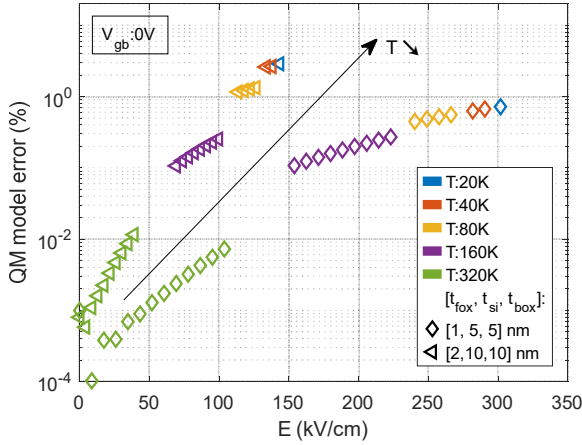


Fig. 5 QM model error versus electric field E at different temperatures T for a two different FDSOI stack.

(similar to [15]) for 300 randomly generated configurations in terms of layer thicknesses and temperature (t_{fox} , t_{si} , t_{box} and T range in [1, 5] nm, [5, 40] nm, [20, 50] nm and [1, 400] K, respectively), considering a {100} silicon orientation (Table I), 15 subband levels (without considering the band broadening at low temperature [16]). We extract Γ_0 from PS1D simulation results, inverting (12):

$$\Gamma_0 = \frac{12\phi_T^2 \ln(10) dSS^{-1}}{k_{eq}^2} \Big|_{dV_{g\Delta}=0} \quad (16)$$

Compared to these extractions, the predicted Γ_0 is remarkably accurate in the whole $t_{si}^2 T$ range (Fig. 2). In particular, it predicts the convergence to $\Gamma_0 = 1$ in the classical limit at high $t_{si}^2 T$. The asymptote $\Gamma_0 = \left(\frac{15-\pi^2}{\pi^4}\right) \frac{k_B m_{z,up}}{\hbar^2} t_{si}^2 T$ at low $t_{si}^2 T$ describes the regime where only the lowest energy level contributes to the charge. The deviation from this asymptote occurs when the other levels start to be significantly filled, around $t_{si}^2 T = 4 \cdot 10^{-15} \text{ m}^2 \text{K}$. The truncation from $n = 20$ of the infinite sum in (13) ensures a Γ_0 error less than 1% in the studied $t_{si}^2 T$ range.

Because SS spreads over a wide range with T , and in order to ease the comparison between results, we compute

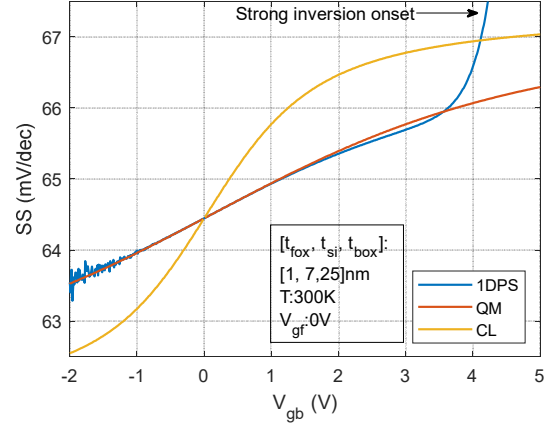


Fig. 6 SS versus V_{gb} at $V_{gf} = 0$ for a typical FDSOI stack, extracted from PS1D results and predicted by QM and CL models.

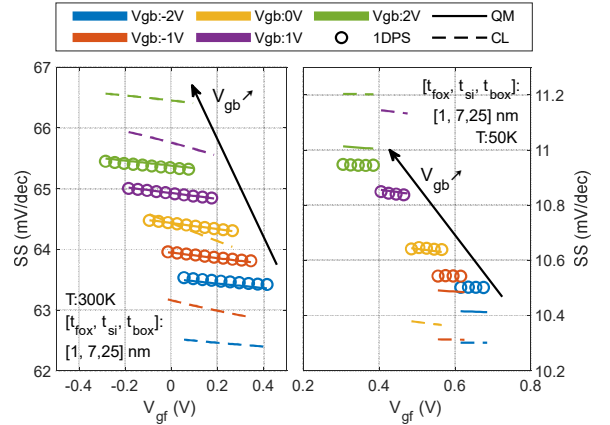


Fig. 7 SS versus V_{gf} at different V_{gb} for a typical FDSOI stack, extracted from PS1D results and predicted by QM and CL models at 300K and 50K.

δSS defined as the relative deviation of SS from its value at null electric field:

$$\delta SS(V_{g\Delta}) = \frac{SS(V_{g\Delta}) - SS|_{V_{g\Delta}=0}}{SS|_{V_{g\Delta}=0}} \quad (17)$$

We then compare predicted δSS from CL and QM models and extracted δSS from PS1D simulation for a typical FDSOI stack (Fig. 3). At the vicinity of $V_{g\Delta} = 0$, the QM model matches almost exactly the 1DPS results in all the temperature range, whereas the CL model deviates at a rate of 0.1 to 10 %/V, depending on temperatures.

The comparison extension to larger $V_{g\Delta}$ (Fig. 4.a) shows the accuracy degrades when the electric field increases (Fig. 4.b), which is expected from the unmet LEF condition. However the QM model error is still the lowest, although the CL model already demonstrates high accuracy. We notice that shrinking the geometry improves the prediction (Fig. 5). The intrinsic QM model accuracy when few subband are filled – which occurs when t_{si} or T are small – seems to compensate the accuracy degradation due to higher electric field. Back biasing (i.e. $V_{gb} \neq 0$) highlights even more the prediction enhancement coming from the QM model (Fig. 6), in particular at low temperatures (Fig. 7).

Other than the $V_{g\Delta}$ scaling depicted in (15), the QM correction can also be implemented using the “dark spaces” approach [17] which consists on changing the FDSOI stack layer effective thicknesses [8]. In the present case, it implies

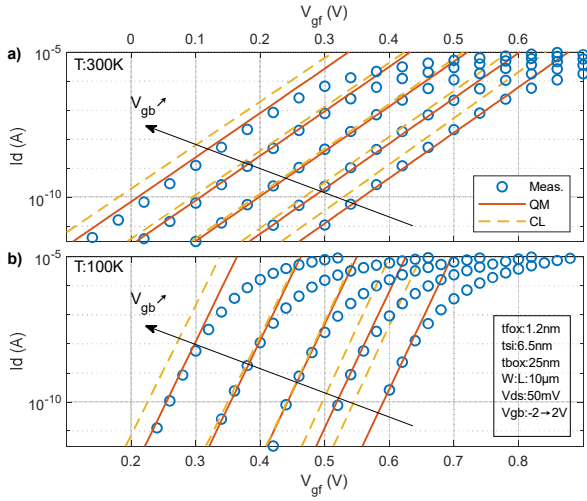


Fig. 8 I_d versus V_{gf} for different back biasing V_{gb} at a) 300K and b) 100K, from LETI measurements and from QM and CL model predictions (assuming diffusion current only, constant mobility and considering a front and back gate flat band voltage shifts of $E_{1,up}^{(0)}$ in the QM model).

the following transformations:

$$\begin{cases} t_{si} \rightarrow t_{si}^{QM} = t_{si}(1 - 2\rho) & (18.a) \\ t_{fox} \rightarrow t_{fox}^{QM} = t_{fox} + \rho t_{si} \varepsilon_{fox} / \varepsilon_{si} & (18.b) \\ t_{box} \rightarrow t_{box}^{QM} = t_{box} + \rho t_{si} \varepsilon_{box} / \varepsilon_{si} & (18.c) \end{cases}$$

$$\rho = (1 - \sqrt{\Gamma_0})/2 \quad (19)$$

It allows rewriting (15) as:

$$SS_{QM}(V_{g\Delta}, k_f, k_b, k_{eq}) \equiv SS_{CL}(V_{g\Delta}, k_f^{QM}, k_b^{QM}, k_{eq}^{QM}) \quad (20)$$

These rescaled thicknesses introduction in the Q_i model (2), substantially improves experimental subthreshold drain current predictions when $V_{gb} \neq 0V$, in particular at low temperatures (Fig. 8).

Although no interface fixed charges or traps have been introduced in the presented cases, their effects could be implemented in the QM model in the same way as for the CL model by properly rescaling gates flat band voltages and oxide capacitances [18]. Similarly, as for CL model, the cryogenic subthreshold swing saturation can be introduced by a temperature pinning [19], [20].

IV. CONCLUSION

The presented FDSOI MOSFET SS model accounting for LEF QM effect predicts extractions from 1DPS simulations with an unprecedented accuracy, in a wide range of temperatures and biases. Although the already high accuracy of the CL model limits the prediction enhancement, the proposed SS QM model provides the appropriate LEF SS QM correction. Implemented with a “dark space” approach, the corresponding FDSOI stack layer thickness rescalings allow a better prediction of the V_{gb} dependence of experimental FDSOI MOSFET subthreshold drain current.

REFERENCES

[1] G. Baccarani and S. Reggiani, “A compact double-gate MOSFET model comprising quantum-mechanical and nonstatic effects,” *IEEE Trans. Electron Devices*, vol. 46, no. 8, pp. 1656–1666, Aug. 1999, doi: 10.1109/16.777154.

[2] L. Ge and J. G. Fossum, “A novel compact model of quantum effects in scaled SOI and double-gate MOSFETs,” in *2000 IEEE International SOI Conference. Proceedings (Cat. No.00CH37125)*, Oct. 2000, pp. 114–115. doi: 10.1109/SOI.2000.892796.

[3] L. Ge and J. G. Fossum, “Analytical modeling of quantization and volume inversion in thin Si-film DG MOSFETs,” *IEEE Trans. Electron Devices*, vol. 49, no. 2, pp. 287–294, Feb. 2002, doi: 10.1109/16.981219.

[4] Q. Chen, L. Wang, and Meindl, “Quantum mechanical effects on double-gate MOSFET scaling,” in *2003 IEEE International Conference on SOI*, Oct. 2003, pp. 183–184. doi: 10.1109/SOI.2003.1242945.

[5] W. Wang, H. Lu, J. Song, S.-H. Lo, and Y. Taur, “Compact modeling of quantum effects in symmetric double-gate MOSFETs,” *Microelectron. J.*, vol. 41, no. 10, pp. 688–692, Oct. 2010, doi: 10.1016/j.mejo.2010.05.007.

[6] V. P. Trivedi and J. G. Fossum, “Quantum-mechanical effects on the threshold voltage of undoped double-gate MOSFETs,” *IEEE Electron Device Lett.*, vol. 26, no. 8, pp. 579–582, Aug. 2005, doi: 10.1109/LED.2005.852741.

[7] S. Khandelwal *et al.*, “BSIM-IMG: A Compact Model for Ultrathin-Body SOI MOSFETs With Back-Gate Control,” *IEEE Trans. Electron Devices*, vol. 59, no. 8, pp. 2019–2026, Aug. 2012, doi: 10.1109/TED.2012.2198065.

[8] T. Poiroux *et al.*, “Leti-UTSOI2.1: A Compact Model for UTBB-FDSOI Technologies - Part II: DC and AC Model Description,” *IEEE Trans. Electron Devices*, vol. 62, no. 9, pp. 2760–2768, Sep. 2015, doi: 10.1109/TED.2015.2458336.

[9] F. Stern, “Self-Consistent Results for n -Type Si Inversion Layers,” *Phys. Rev. B*, vol. 5, no. 12, pp. 4891–4899, Jun. 1972, doi: 10.1103/PhysRevB.5.4891.

[10] G. Ghibaudo and G. Pananakakis, “Analytical expressions for subthreshold swing in FDSOI MOS structures,” *Solid-State Electron.*, vol. 149, pp. 57–61, Nov. 2018, doi: 10.1016/j.sse.2018.08.011.

[11] H.-C. Han, F. Jazaeri, Z. Zhao, S. Lehmann, and C. Enz, “An improved subthreshold swing expression accounting for back-gate bias in FDSOI FETs,” *Solid-State Electron.*, vol. 202, p. 108608, Apr. 2023, doi: 10.1016/j.sse.2023.108608.

[12] J. P. Mazellier *et al.*, “Threshold voltage in ultra thin FDSOI CMOS: Advanced triple interface model and experimental devices,” in *2008 9th International Conference on Ultimate Integration of Silicon*, Mar. 2008, pp. 31–34. doi: 10.1109/ULIS.2008.4527135.

[13] T. Poiroux *et al.*, “Leti-UTSOI2.1: A Compact Model for UTBB-FDSOI Technologies - Part I: Interface Potentials Analytical Model,” *IEEE Trans. Electron Devices*, vol. 62, no. 9, pp. 2751–2759, Sep. 2015, doi: 10.1109/TED.2015.2458339.

[14] F. M. Fernández and E. A. Castro, “Exact perturbation theory for quantum-mechanical systems within boxes,” *Phys. Rev. A*, vol. 46, no. 11, pp. 7288–7291, Dec. 1992, doi: 10.1103/PhysRevA.46.7288.

[15] T. Ouisse, “Self-consistent quantum-mechanical calculations in ultrathin silicon-on-insulator structures,” *J. Appl. Phys.*, vol. 76, no. 10, pp. 5989–5995, Nov. 1994, doi: 10.1063/1.358382.

[16] H. Bohuslavskiy *et al.*, “Cryogenic Subthreshold Swing Saturation in FD-SOI MOSFETs Described With Band Broadening,” *IEEE Electron Device Lett.*, vol. 40, no. 5, pp. 784–787, May 2019, doi: 10.1109/LED.2019.2903111.

[17] A. Pacelli, A. S. Spinelli, and L. M. Perron, “Carrier quantization at flat bands in MOS devices,” *IEEE Trans. Electron Devices*, vol. 46, no. 2, pp. 383–387, Feb. 1999, doi: 10.1109/16.740906.

[18] N. Rostand *et al.*, “Total Ionizing Dose Effects in FDSOI Compact Model for IC Design,” *IEEE Trans. Nucl. Sci.*, vol. 66, no. 7, pp. 1628–1633, Jul. 2019, doi: 10.1109/TNS.2019.2911429.

[19] G. Ghibaudo, M. Aouad, M. Casse, S. Martinie, T. Poiroux, and F. Balestra, “On the modelling of temperature dependence of subthreshold swing in MOSFETs down to cryogenic temperature,” *Solid-State Electron.*, vol. 170, p. 107820, Aug. 2020, doi: 10.1016/j.sse.2020.107820.

[20] G. Pahwa, P. Kushwaha, A. Dasgupta, S. Salahuddin, and C. Hu, “Compact Modeling of Temperature Effects in FDSOI and FinFET Devices Down to Cryogenic Temperatures,” *IEEE Trans. Electron Devices*, vol. 68, no. 9, pp. 4223–4230, Sep. 2021, doi: 10.1109/TED.2021.3097971.